applied sciences

MDPI

Article

Comparison of Feedforward Perceptron Network with LSTM for Solar Cell Radiation Prediction

Tugba Ozdemir [1,2,*], Fatma Taher [3], Babajide O. Ayinde [2], Jacek M. Zurada [2,4] and Ozge Tuzun Ozmen [1,5]

[1] Department of Physics, Faculty of Arts and Sciences, Duzce University, Konuralp Yerleskesi, Duzce 81620, Turkey; ozge.ozmen@bakircay.edu.tr
[2] Electrical and Computer Engineering, University of Louisville, Louisville, KY 40292, USA; babajide.ayinde@echonous.com (B.O.A.); jacek.zurada@louisville.edu (J.M.Z.)
[3] Department of Computing & Applied Technology & Assistant Dean for Research and Out Reach in the College of Technological Innovation, Zayed University, Dubai 19282, United Arab Emirates; fatma.taher@zu.ac.ae
[4] Information Technology Institute, University of Social Science, 90-113 Łódz, Poland
[5] Department of Fundamental Sciences, İzmir Bakırçay University, Izmir 35665, Turkey
* Correspondence: tugbaozdemir238@gmail.com

Abstract: Intermittency of electrical power in developing countries, as well as some European countries such as Turkey, can be eluded by taking advantage of solar energy. Correct prediction of solar radiation constitutes a very important step to take advantage of PV solar panels. We propose an experimental study to predict the amount of solar radiation using a classical artificial neural network (ANN) and deep learning methods. PV panel and solar radiation data were collected at Duzce University in Turkey. Moreover, we included meteorological data collected from the Meteorological Ministry of Turkey in Duzce. Data were collected on a daily basis with a 5-min interval. Data were cleaned and preprocessed to train long-short-term memory (LSTM) and ANN models to predict the solar radiation amount of one day ahead. Models were evaluated using coefficient of determination (R^2), mean square error (MSE), root mean squared error (RMSE), mean absolute error (MAE), and mean biased error (MBE). LSTM outperformed ANN with R^2, MSE, RMSE, MAE, and MBE of 0.93, 0.008, 0.089, 0.17, and 0.09, respectively. Moreover, we compared our results with two similar studies in the literature. The proposed study paves the way for utilizing renewable energy by leveraging the usage of PV panels.

Keywords: renewable energy; solar energy; artificial neural network; deep learning; LSTM; radiation prediction

check for updates

Citation: Ozdemir, T.; Taher, F.; Ayinde, B.O.; Zurada, J.M.; Tuzun Ozmen, O. Comparison of Feedforward Perceptron Network with LSTM for Solar Cell Radiation Prediction. *Appl. Sci.* **2022**, *12*, 4463. https://doi.org/10.3390/app12094463

Academic Editor: Luis Hernández-Callejo

Received: 9 January 2022
Accepted: 21 March 2022
Published: 28 April 2022

1. Introduction

1.1. Background

In recent years, the role of energy in the life standard of human beings has been vitally important [1–3]. As the human population increases, energy demands increase exponentially [2–5]. Researchers demonstrate that the energy demand is anticipated to be approximately 1.5–3 times by 2050 [2,6,7]. Given that fact, we can anticipate that fossil fuels such as petroleum, natural gas, and coal, which are the traditional energy sources, will be depleted very soon. One more reason to switch to renewable energy is how harmful the fossil fuels are to the environment [4,8]. It should be emphasized that consumption of energy from fossil fuels is increasing CO_2 (carbon dioxide) and greenhouse gas (GHG) emissions all over the world [6,9]. Increasing GHGs cause a rising atmospheric temperature of the Earth's surface [7–13]. With this concern, renewable energy has come into question for the last century [2–5,7–13].

Alternatively, solar energy, which is among renewable energy sources, is abundant and environmentally friendly, and photovoltaic (PV) technology has provided development and discovery for both rural and urban choices on a global scale [5,9–17]. The history of modern PV energy is based on Alexandre Becquerel's 1839 observation of the photoelectric effect [13–17]. However, after the 1990s, studies on PV energy rapidly improved [5,18]. In addition, annual PV solar energy exceeded that of wind power for the first time and reached about 70 GW, and was even 50% higher than in the previous year [18]. The global solar PV capacity reached at least 303 GW (48% compared to 2015) at the end of 2016 [18,19]. Furthermore, reports from the world's solar photovoltaic electricity supplies anticipate that PV technologies will increase to 345 GW and 1081 GW by 2020 and 2030, respectively [1,5,12,19].

The rapid expansion of PV systems does not only provide economic benefits to the electrical systems but also contributes to the reduction of global heating problems [19]. Although a solar PV system can operate by itself, a grid-connected system is required in order to reliably evaluate the electricity generation system [20,21]. Nonetheless, the instability of weather conditions and solar radiation lead to the instability of the power produced by PV panels, which causes a lot of problems in the control and operation of grid-connected PV panels [22–24]. To solve the instability problems, researchers have been developing methods to predict the output power of PV panels based on historical data and meteorological data [25,26]. Recently, artificial neural networks (ANNs) have been used to improve the prediction power of PV panels' output. ANNs have been utilized to solve further problems such as estimating radiation amount, solar power, and ambient temperature parameters [26,27]. ANNs have been applied for the modeling, identification, optimization, prediction, and control of complex systems. Hence, several studies report using ANNs in solar radiation modeling and prediction. Most of those studies utilized the geographical coordinate and meteorological data such as relative humidity, air temperature, pressure, sunshine duration, etc. as an input to the ANNs for estimating of global solar radiation [26,27]. In the following subsection, we go through some of the relevant literature to demonstrate the attempts to predict solar radiation using machine learning.

1.2. Literature Review

Table 1 covers the literature review section of this paper. In the following table, we mention the authors, cities at which the data was collected, the research aim, date when the data was acquired, the models utilized for achieving the research aim, and last but not least, the performance of each model.

Table 1. Literature review.

Authors and Reference	Case Study	Research Objective	Data	Models Used	Performance of Models
A. Mellit et al. [28]	Trieste, Italy	Estimate the amount of solar radiation for 24h using grid-connected photovoltaic plants (GCPV).	From July 1st 2008 to May 23rd 2009 for solar radiation, from November 23rd 2009 to January 24th 2010 for air temperature data.	ANN	The correlation coefficient was 98–99% for sunny days and 94–96% for cloudy days.
C. Voyant et al. [29]	Mediterranean Sea: Ajaccio, Bastia, Montpellier, Marseille, and Nice	Estimate the global solar radiation with two models.	Data on an hourly basis from October 2002 to December 2008 and from French meteorological organization.	• ARMA/ANN hybrid model, • the numerical weather prediction model (ALADIN).	• The nRMSE for hybrid model MLP/ARMA was 14.9% compared to 26.2% for the naïve persistence predictor.
A. Sozen et al. [30]	17 different cities in Turkey	• Estimate the solar potential based on geographic coordinates meteorological data (and the corresponding month) as inputs to the network.	The data were collected from 17 meteorological stations between 2000 and 2002.	ANNs	• MAPE (mean absolute percentage error) was found to be less than 6.735%. • R^2 was found to be about 99.893% for the testing stations.
A. Mellit et al. [31]	In Tahifet, south Algeria	They presented an application of an RNN-based approach to estimate the daily electricity generation of a photovoltaic power system (PVPS).	The measured weather data and the output of electrical signals (voltage and current) were recorded at the PVPS station in Algeria from 1992 to 1997.	ANN and RNN	• MAPE was lower than 5.5%. • The correlation coefficient ranged between 95 and 97%.
J. M. S. de Araujo [32]	Gifu, Japan	For hourly solar radiation prediction.	• The dataset from the NOMADS website. • Three years' data of solar radiation from 1st January 2014 to 31st December 2016 for LSTM.	LSTMWRF (weather research and forecasting)	• LSTM algorithm was 310 W m^{-2} higher compared to 210 W m^{-2} from the WRF model. • The error of WRF was 19% lower compared to 28% of LSTM for the nRMSE error metric.

Table 1. *Cont.*

Authors and Reference	Case Study	Research Objective	Data	Models Used	Performance of Models
A. Alzahrani et al. [33]	Canada	Estimate solar irradiance using a deep neural network.	The data were recorded for four days, from Canada's natural sources.	• Deep recurrent neural networks (LSTM) • Support vector regression (SVR) • Feedforward neural networks (FNN)	RMSE: • LSTM = 0.086 • SVR = 0.11 • FNN = 0.16 MBE: • LSTM = 0.004 • SVR = 0.0042 • FNN = 0.005
A. Rai et al. [34]	Three different geographical regions in different climatic zones.	For midterm solar radiation estimation.	The data came from three different geographical regions in different climatic zones between 2014 and 2015 years.	• A convolution neural network (CNN) • Bi-direction long-short-term memory (BiLSTM)-based hybrid deep learning (DL) model.	For CNN-BiLSTM • R^2 = 0.924 • MAE = 0.0397
J. H. Yousif et al. [35]	Many different locations around the world.	Some different ANN techniques to estimate the photovoltaic thermal (PV/T) energy.	Data were taken from 2008–2017 for locations with different latitudes and climates.	Some models: • Bayesian neural network (BNN) • RNN • Generalized feed-forward (GFF) • MLP • LSTM	They gave error results such as MAPE, MSE, RMSE, MBE, MPE, and R^2.
Y. Jung et al. [36]	South Korea	To predict the amount of PV solar power.	The data were obtained from 164 PV plants for 63 months.	RNN-LSTM	• RMSE = 7.416% • MAPE = 10.805% for the testing data
M. Mishra et al. [37]	Urbana Champaign, Illinois	To forecast a short-term solar power using various time intervals (1 day, 15 days, 30 days, 60 days ahead forecasting).	The datasets from February 2016–August 2017 and September 2017–October 2017.	• Wavelet transform (WT)-based DLM • LSTM-Dropout • Linear regression (LR), • Some other models	They gave error results such as RMSE, MAE, MAPE, and R^2.
S. Ghimire et al. [38]	Australia	Propose a convolutional long-short-term memory (CLSTM) neural network hybrid model to predict half-hourly global solar radiation (GSR).	Data from 1 January 2006 to 31 August 2018.	Some models: • Convolutional neural networks (CNN) • LSTM • Gated recurrent unit (GRU).	• Relative root mean square error (≈1.515%) • Mean absolute percentage error (≈4.672%) • Absolute percentage bias (≈1.233%)
D. Lee et al. [39]	Gumi city in South Korea	Build three different deep learning models to predict the solar power output of PV panels.	Data were a PV power output dataset for 39 months (from 1 June 2013 to 31 August 2016) from a PV operator located in Gumi city in South Korea.	• ANN • DNN LSTM	LSTM-based model performs better by more than 50% compared to the conventional statistical models in terms of mean absolute error.
Z. Pang et al. [40]	Tuscaloosa, Alabama, United States	Create two models using a shallow ANN and an RNN to estimate the solar radiation.	The data utilized wereonly meteorologicaldata from a localweather station in Tuscaloosa, Alabama, United States	• A shallow ANN an RNN	They gave error results of RMSE and NMBE for both models.

1.3. The Proposed Study

Based on the aforementioned literature review, we found that data from PV panels and/or meteorological data are utilized to predict solar radiations. The highest achievable results were found by deep learning techniques [28,31,36–44]. Therefore, we designed our experiment based on shallow and deep learning models. The motivation behind the proposed study was the irregularity of energy delivery in Duzce city in Turkey, which may exist in similar cities around the world. We utilized both PV historical data, which was collected from the city of Duzce in Turkey for the period between 2014 to 2018, as well as the daily meteorological data for the same period. In the proposed study, we compared between a deep ANN and an LSTM model in terms of predicting the solar radiation in the city of Duzce in Turkey on daily basis. We performed hyperparameter optimization at predefined hyperparameter values for both the networks, ANN and LSTM. Selecting a deep learning architecture to perform an accurate prediction of the solar radiation amount is crucial for the system operators to reduce costs and uncertainties [17,41–44]. The main contributions of the proposed work can be summarized as: (i) conducting a comparison between the performance of the most common deep learning models in the literature, (ii) building an LSTM to accurately predict the solar radiation at the city of Duzce in Turkey with the potential to be generalized to more cities around the world, and (iii) conducting a comparison between our results in terms of the coefficient of determination (R^2), root mean squared error (RMSE), mean biased error (MBE), and mean absolute error (MAE).

2. Materials and Methods

2.1. Dataset

The solar data, which were utilized in the current study, were collected from three different types of grid-connected PV panels. The PV panels were installed on the top roof of the University of Duzce Scientific and Technological Research and Application Center (DUBIT) by Duzce University Clean Energy Resources Application and Research Center (DÜTEM) in 2013 in Turkey. The geographic location of the center panel is 40°54′14.7″ N and 31°10′56.7″ E. Figure 1 shows the three different PV solar panels of schemas in DUBIT in Duzce University in Duzce.

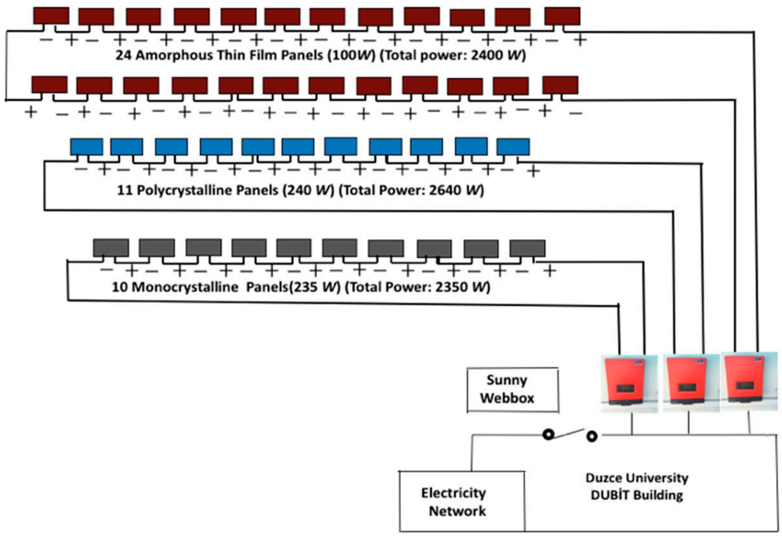

Figure 1. Three different PV solar panels of schemas in DUBIT in Duzce.

As shown in Figure 1, the first type of panels used (P1) is an amorphous thin film silicon panel. A single P1 panel has the power of 100 W. In the proposed study, 24 P1 panels were utilized. The 24 P1 panels were structured in the form of a matrix with two rows and twelve columns (2 × 12). The total output power generated by the (P1) panels matrix equals 2400 W. The second type of panel (P2) is a polycrystalline silicon panel. A single P2 has a solar panel power of 240 W. Eleven P2 panels were utilized in the current study. The 11 (P2) panels were placed as a single row. That row produces a total power output of 2400 W. The third type of panel (P3) is a monocrystalline silicon panel. P3 produces a solar panel power of 235 W. Ten P3 panels were placed in a single row. Those have a total power output 2350 W. That system of panels (P1, P2, and P3) has been recording data every 5 min since 2013. Output power is recorded for each panel. Average temperature, radiation amount, and average atmospheric temperature were recorded for all panels.

Table 2 demonstrates an example of the recorded data recorded from P1, P2, and P3. Therefore, for every day, there are 288 rows of data and 6 columns (3 columns denote the output power for each panel type (kWh), 1 column denotes average atmospheric temperature ($\hat{A}$ °C), 1 column denotes radiation amount (W/m^2), and 1 column denotes panel temperature ($\hat{A}$ °C). Rows are indexed with the time of acquisition. Moreover, meteorological data were recorded on daily basis. Thus, for every 288 rows of panels' data, there is a corresponding row of meteorological data. Meteorological data acquired were as follow: daily average relative humidity, daily sunshine time, and daily average cloudiness. Meteorological data were recorded by the Ministry of Metrology in Turkey. The rationale behind using the meteorological data is to include any factor that might be affecting the radiation amount detected by the panels. Some of the meteorological data is presented in Table 3.

Table 2. Data from PV panels recorded every five minutes in DUBIT.

Dates dd.MM.yyyy HH:mm	P_1 Amorphous Thin-Film Silicon (kWh)	P_2 Polycrystalline Silicon (kWh)	P_3 Monocrystalline Silicon (kWh)	Average Atmospheric Temperature (Â °C)	Radiation Amounts (W/m^2)	Panels Temperature (Â °C)
01.01.2014 11:50	454.81	600.56	613.59	7.40	55.00	7.70
01.01.2014 11:55	454.82	600.57	613.60	7.40	56.00	7.70
01.01.2014 12:00	454.83	600.58	613.61	7.40	56.00	7.70
01.01.2014 12:05	454.84	600.58	613.62	7.40	54.00	7.60
01.01.2014 12:10	454.84	600.59	613.62	7.50	53.00	7.60
01.01.2014 12:15	454.85	600.60	613.63	7.50	53.00	7.70
01.01.2014 12:20	454.86	600.61	613.64	7.50	56.00	7.70
01.01.2014 12:25	454.87	600.62	613.65	7.60	56.00	7.80
01.01.2014 12:30	454.88	600.62	613.65	7.50	56.00	7.80

Table 3. An example of daily average cloudiness from meteorological data in the Turkish State Meteorological Service (the numbers indicate rate of average cloudiness).

	Months											
Days	**Jan.**	**Feb.**	**Mar.**	**Apr.**	**May**	**Jun.**	**Jul.**	**Aug.**	**Sept.**	**Oct.**	**Nov.**	**Dec.**
1	8.0	7.0	6.4	1.5	4.6	6.2	4.4	2.5	5.0	1.2	7.0	7.7
2	7.0	1.1	6.9	4.4	5.2	5.8	4.1	5.2	3.8	2.9	7.0	7.0
3	7.0	0.0	5.9	4.3	4.2	6.0	5.3	6.8	5.4	5.7	3.7	6.5
4	6.4	3.1	6.7	2.7	6.1	6.0	6.1	5.2	4.7	7.0	0.8	6.3
5	4.6	0.7	4.6	5.7	6.3	7.0	4.0	4.3	6.8	5.5	1.9	7.2
6	5.4	0.9	4.3	5.8	6.8	7.0	0.6	1.9	6.3	6.7	0.8	6.4
7	3.6	0.2	3.8	5.3	5.4	6.3	1.1	6.1	3.8	3.8	0.5	6.2
8	0.0	0.6	7.9	6.8	6.7	6.3	1.6	5.6	5.4	3.0	3.0	6.4
9	7.6	5.7	8.0	0.8	6.8	4.9	0.0	5.8	4.6	6.6	5.4	6.8
10	8.6	6.4	8.0	1.2	6.6	3.0	1.9	2.7	5.0	4.8	5.9	6.8

Table 3 shows an example of 10 days' data of the meteorological data that were acquired from the Meteorological Ministry of Turkey in 2014 in Duzce, Turkey. Rows represents days, columns represent months, and the values in each cell represent the average cloudiness on that day in that month and recorded average daily cloudiness for 12 months of the year. Similar tables are given for the other meteorological data. Meteorological data corresponding to 4 years from 2014 to 2018 were utilized in the current study [45].

Data were cleaned by removing rows with missing values, then all the data were aggregated in a single table containing the meteorological data along with the panels' data. Python 3.7 and pandas were utilized for data cleaning and manipulation.

2.2. Deep Neural Network Approaches

In this section, we present the shallow ANN and deep ANN architectures used for forecasting of solar radiation amount as an output, including conventional multi-layer deep ANN, sequential model, recurrent neural network, and long-short-term memory.

2.2.1. Conventional Deep ANN/Multilayer Perceptron (MLP)

Multilayer perceptron was introduced by Rosenblatt in 1958 as the basic type of neural network and consists of a number of perceptron [46–59]. There is an input layer to receive the data and there is an output layer that determines and predicts the output value in multilayer perceptron. Between the input and output layers, there is a selected number of hidden layers, which is the main processing engine of MLP [42–46,56–59].

As shown in Figure 2, MLP is a simple neural network. Equation (1) is used to calculate the output of a single perceptron or neuron [46,59].

$$output = f\left(\sum_{i}^{inputs}(x_i.w_i + b_i)\right), \quad (1)$$

where x_i is the input of the neuron, w_i is the weight on each connection to the neuron, b_i is the bias, and $f(.)$ is the activation function, for instance, the tanh activation function [16,47,59].

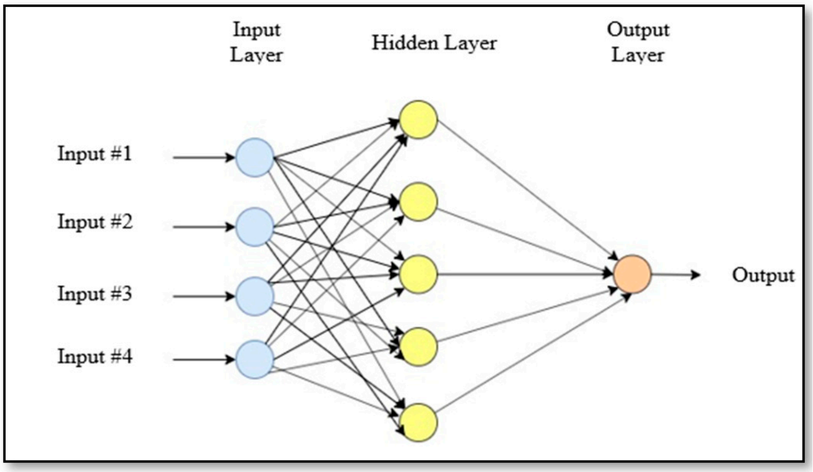

Figure 2. Multilayer perceptron network with single output.

2.2.2. Recurrent Neural Network (RNN)

RNNs are conventional neural networks consisting of one or more feedback loops [47]. RNNs have the ability to utilize their input memory to process entries [48]. In conventional neural networks, all inputs and outputs are considered to be independent of each other. This means that the output is not fed back to the network as an input; however, in the case of RNNs, output can be fed again with the input to be considered in future decisions [47,48]. RNNs' basic architecture is shown in Figure 3.

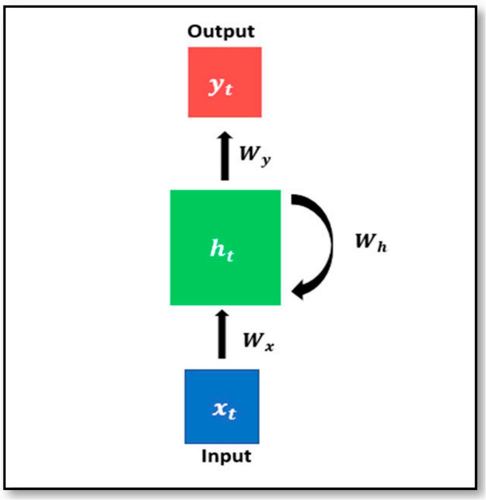

Figure 3. Basic recurrent neural network (RNN).

In Figure 3, the RNN consists of input (x_t), hidden state (h_t), and outputs (y_t). W_x, W_y, and W_h are weight matrices. The most important part of RNN is the hidden state (h_t), which is a vector that can also have an arbitrary dimension [48].

$$h_t = F_w\ (h_{t-1},\ x_t), \tag{2}$$

$$h_t = tanh\left(W_h h_{(t-1)}\ + W_x x_t\right), \tag{3}$$

$$y_t = W_y h_t, \tag{4}$$

Figure 3 also shows the relationship between functions in RNN. In the functions, $h_{(t-1)}$ of previous hidden state contains information from the previous time step; F_w is an activation function as shown Equation (3) [47,48].

2.2.3. Long-Short-Term Memory (LSTM)

LSTM is based on the RNN architecture. It is a model designed to expand the RNN memory [45,46]. This memory has the ability to store information over an arbitrary length of time. There are three gates, which are the input, output, and forget gate, to control the information flow into and out of the neuron's memory [48–51]. Those three gates get the same input as the input neuron. Furthermore, each gate possesses an activation function [41,48,52].

Figure 4 shows the figuration of LSTM at time t. Mathematically, LSTM can be described using the following functions [50–58].

$$f_t = g\left(W_f\, x_t + U_f\, h_{t-1} + b_f\right), \tag{5}$$

$$i_t = g\,(W_i\, x_t + U_i\, h_{t-1} + b_i), \tag{6}$$

$$k_t = tanh\,(W_k\, x_t + U_k\, h_{t-1} + b_k), \tag{7}$$

$$c_t = f_t\, c_{t-1} + i_t\, k_t, \tag{8}$$

$$o_t = g\,(W_o\, x_t + U_o\, h_{t-1} + b_0), \tag{9}$$

$$h_t = o_t\, tanh\,(c_t), \tag{10}$$

where x_t is the input vector at time t and g is an activation function (sigmoid, tanh, or ReLU). W and U are weight matrices, and b is the bias vector. h_t and c_t are output and cell state vector at time t. f_t has been used for remembering old information and it has been used for getting new information [38,49,50,52].

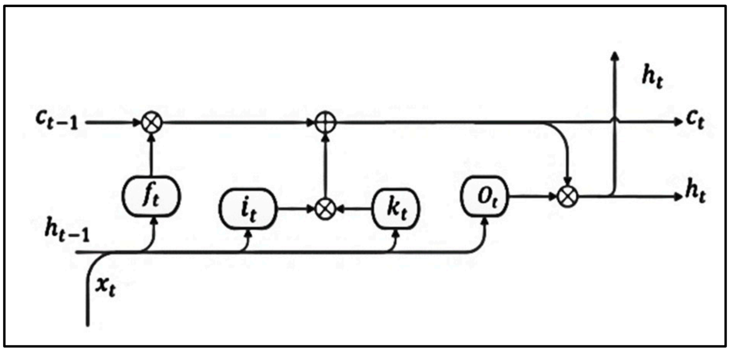

Figure 4. Long-short-term memory (LSTM) at time t.

2.3. Activation Functions

Activation functions are used to add the non-linearity behavior of the ANN [53–56]. Without the activation function, the output of each layer of the ANN would just be the output of a linear model with number of parameters equal to the number of the neurons in each layer [54,55]. Consequently, activation functions increase the overall performance of the ANN and add a nonlinear behavior to it, depending on the behavior of the activation function itself. Thus, if activation functions are not applied on the ANN, the ANN usually has limited performance and acts as a linear regression model [54,55,57,59].

Figure 5 shows the basic structure of the activation function, where x = inputs, w = weights, $f(\Sigma)$ = activation functions, and y = outputs [54,55].

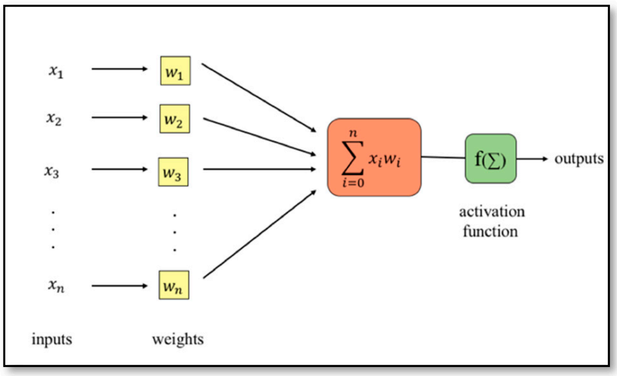

Figure 5. Structure of neural networks with activation function.

The most common activation functions are hyperbolic tangent function, sigmoid function, linear function, ReLU (rectified linear unit) function, leaky-ReLU function, softmax function, and swish (a self-gated) function [55,58,59].

In this work, we use the hyperbolic tangent function (*tanh*) as the activation function for our proposed ANN and DNN models. The tanh function is used for the input and hidden layers.

In hyperbolic tangent function $(-1, 1)$

$$f(x) = tanh(x) = \frac{(e^x - e^{-x})}{(e^x + e^{-x})}, \tag{11}$$

However, the rectified linear unit (ReLU) activation function is utilized in the output layer to provide a non-negative solar radiation predictive value [54–59].

ReLU (rectified linear unit) function $[0, \infty)$

$$f(x) = \begin{cases} 0 \; for \; x < 0 \\ x \; for \; x \geq 0 \end{cases}, \tag{12}$$

3. Experimental Design

3.1. Dataset Description

Panels data and meteorological data of the full dataset were used in this study as detailed in the methodology. Panels log their power reading during the daytime, i.e., sunrise to sunset. From the sunset to sunrise, the panel does not provide any information about their output power; however, we still have data about their average temperature. Therefore, to maximize the information in our data, we filtered out the period between sunset to sunrise which varies between winter and summer. We added the meteorological data, which consisted of cloudiness, relative humidity, and sun time, to the panels' data. Meteorological data were recorded as one sample per day while panels' data were recorded every 5 min. Therefore, we created three new columns for every panel's data file and assigned to those columns the meteorological values for that day by repeating it n times where n is the number of rows/entries in that panel's data file. In this way, we have built a connection between solar data and meteorological data. We used the same epochs numbers and batch size for two models owing to the comparison.

Deep ANN and LSTM were utilized in this study to predict the daily solar radiation. Inputs were amorphous silicon PV panel in kWh, mono silicon PV panel in kWh, poly silicon PV panel in kWh, average atmospheric temperature in °C, average panel temperature in °C, daily average cloudiness, daily average relative humidity (%), and daily sunshine time in hours, and the output was the predicted radiation amount (W/m^2).

Four years' worth of data were utilized in the proposed study. The data were split into 3 years for training and 1 year for testing. Results in terms of mean square error (MSE) were computed for each model. The training set was split further into a training and validation set for both models. Eventually, the two trained models were evaluated using the testing set. The assumption was that the trained model which has been trained on the 3 years of data can then be used to perform the prediction throughout the 4th year with the same range of error. For both models, we concatenated the daily meteorological data to the data acquired from the PV panels. In order to preserve the data acquired by the panel, each daily metrological value was repeated in the rows corresponding to that day. We trained both models using the aggregated data by averaging every 12 rows (=60 min) and predicting the following 48 row's solar radiation (=predicting the solar radiation after 48 h). The data were then normalized between 0 and 1, and the normalized data were used for the learning process.

3.2. Description of the ANN Model

As shown in Figure 6, we created an ANN model for prediction of radiation amounts. Deep ANN was utilized with a structure of 1 input layer of size 8, 2 hidden layers each of size 50, and a single output layer with size 1. Therefore, we utilized only one row to predict the following 48th row.

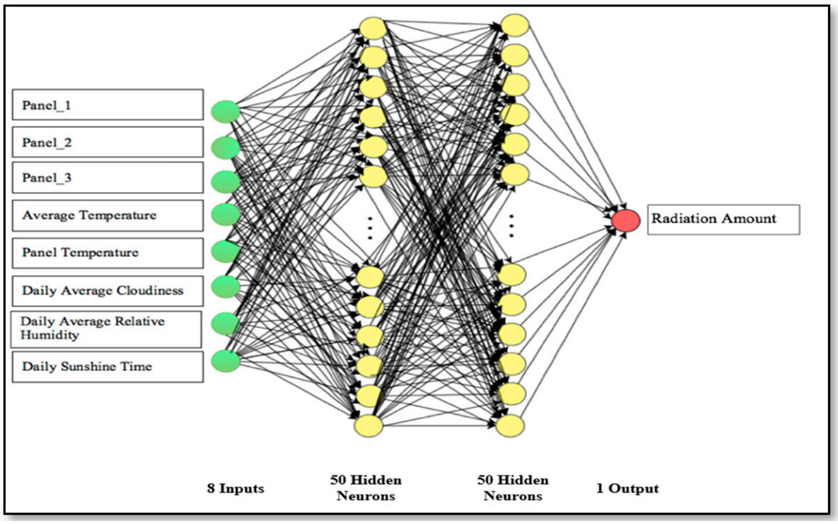

Figure 6. ANN model.

For the model in Figure 6, the tanh function was used as the activation function for the proposed model. Hyperparameter optimization using random grid search was performed on the batch size and the learning rate. Stochastic gradient descent (SGD) was utilized as the optimizing parameter for the deep ANN. The hyperparameters' ranges are specified in the following Table 4.

Table 4. Hyperparameters of the ANN model.

Epochs	500
Batch size	16, 32, 64, 128, 256, 512, 1024
Learning Rate (LR)	[0.0005, 0.05] with step 0.005

Table 4 demonstrates the hyperparameters of the ANN model.

3.3. Description of the LSTM Model

LSTM is an advanced RNN used to specify which feature should be memorized or forgotten when the network is being trained. Therefore, given a sufficient history of features and solar radiation, the LSTM can determine the required history for each feature to provide an accurate solar radiation estimation.

In the proposed LSTM/DNN model, we allowed the LSTM to access up to 30 h in the past in order to predict the solar radiation after 48 h. Hyperparameters optimization via grid search was performed on the hyperparameters shown in Table 5.

Table 5. Hyper parameters of the LSTM model.

Epochs	500
Batch size	16, 32, 64, 128, 256, 512, 1024
n	1, 2, 5, 10, 15, 20, 30 h

The loss function of LSTM was the mean squared error (MSE) and the model was implemented by Keras.

3.4. Error Measures

The performance of the reference methods and the different approaches were evaluated with five different error measures for ANNs. The equation shows the mean-square error (MSE) [50,59].

$$\mathrm{MSE}(x', x) = \frac{1}{N}\sum_{n=1}^{N}(x'_n - x_n)^2 \ , \quad (13)$$

In the equations, x is the measured power time series, $x^{2'}$ is the predicted power time series, and N denotes the number of samples of the time series [47,48,59].

4. Results and Discussion

The training and texting process is shown in Figure 7. Loss function with 500 epochs, batch size of 256 was used for this ANN model.

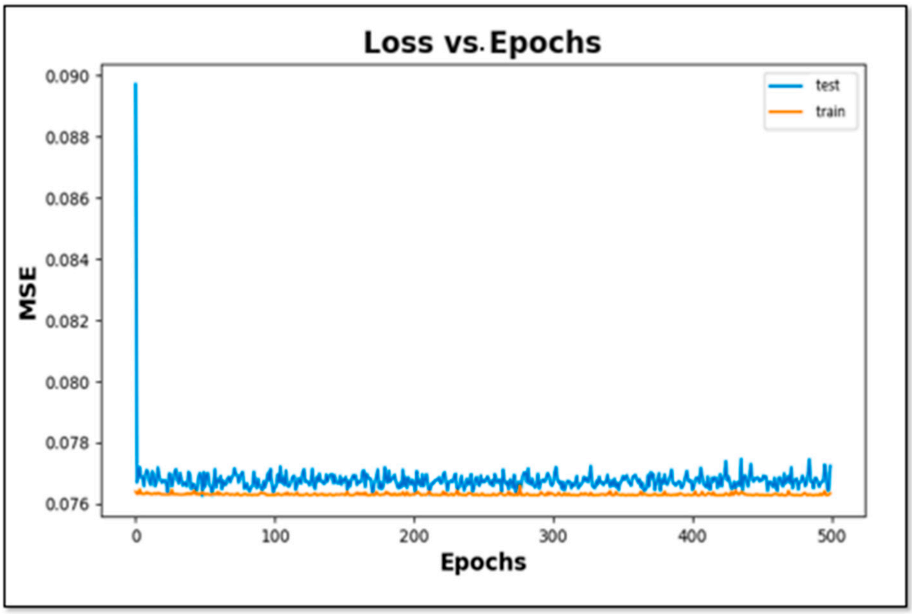

Figure 7. Loss function with 500 epochs for ANN model, batch size of 256.

As shown in Figure 7, the minimum training MSE and minimum testing MSE were 0.0762 and 0.0775, respectively, for the ANN model. The optimum parameters selected for the ANN model were batch size 256 and learning rate 0.01.

Figure 8 shows the graph of training and texting of data with the LSTM model for 500 epochs.

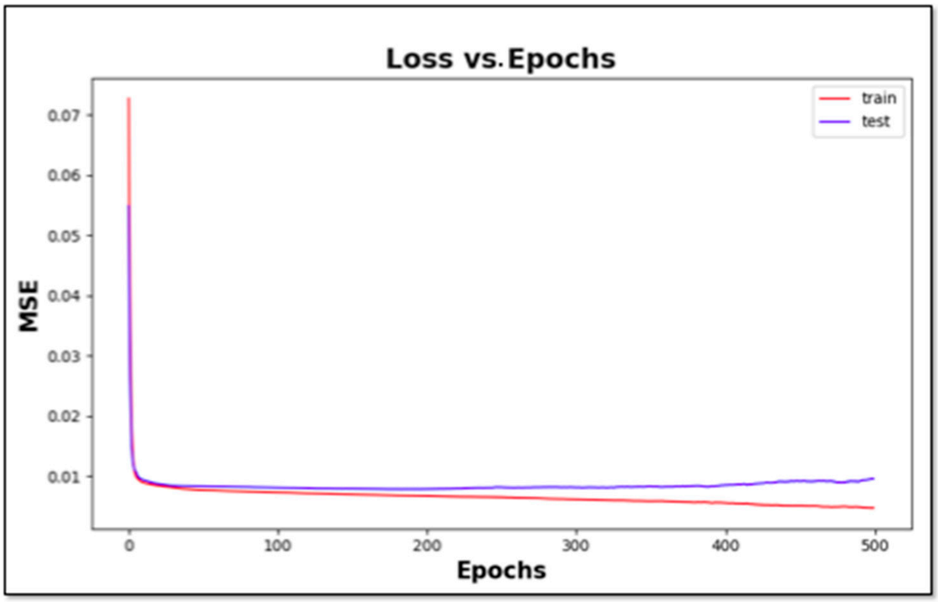

Figure 8. The graph of training and testing of data with LSTM model for 500 epochs.

As demonstrated in Figure 8 for the LSTM model, the minimum training MSE and minimum testing MSE were 0.0049 and 0.0080, respectively. The optimum parameters selected for the ANN model were batch size 256 and past days of 15 h.

Table 6 compares the results obtained by using the ANN model and the LSTM model. Using MSE to calculate the error/loss of the two models, it was found that LSTM improves the results about 18 times in case of training, and about 9 times in case of testing. Since LSTM successfully outperformed ANN by utilizing the data from the previous 15 h, LSTM was the chosen model to test on the 4th year testing data.

Table 6. Error comparison of models after 500 epochs.

Method	MSE	
ANN Model	Minimum training loss	0.0762
	Minimum testing loss	0.0775
LSTM (Deep Learning)	Minimum training loss	0.0049
	Minimum testing loss	0.0080

Figure 9 shows a sample of the prediction performed using the LSTM trained model on 175 days of the 4th year assigned for testing the trained model. Number of days are shown on the horizontal axis versus the normalized solar radiation on the vertical axis. We calculated the coefficient of determination, R^2, along with the MSE for the testing results. R^2 was found to be 0.9365 and MSE was 0.01. In order to demonstrate the significance of our results, we compared our results to similar work in the literature by M. Mishra et al. [37] and U. Agbulut et al. [60]. Moreover, U. Agbulut et al. [60] predicted the solar radiation by using deep learning models for four different cities in Turkey. We averaged the values of their metric scores over the four cities to compare with ours. On the other hand, M. Mishra et al. [37] utilized wavelet transformation on the historical PV solar output at the University of Illinois in Urbana Champaign along with the meteorological data to train LSTM model to perform daily predictions. The authors compared the performance of different ML models to LSTM. Similar to our findings, LSTM outperformed the other models. They trained the models using 18 months of data and tested with one month. It is worth noting that they were performing hourly predictions for 1 day ahead.

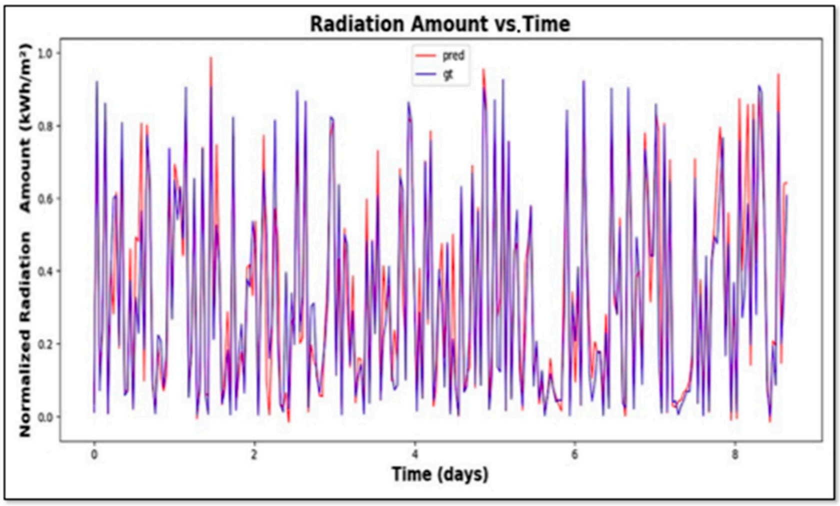

Figure 9. Radiation of 175 days (testing days) as LSTM predicted (blue) versus the ground truth as measured (red).

Table 7 demonstrates the performance of our model with respect to other similar models in the literature. Although we outperformed the other models in terms of R^2, M. Mishra et al. [37] achieved better results in terms of RMSE and MAE. We claim that this higher performance is due to the fact that they performed hourly prediction of the one day ahead and not the whole day. Moreover, we tested on a whole year of data and not only one month.

Table 7. Comparison for ANN.

Metric	[38]	[58]	Proposed Method
R^2	0.426	0.916	0.93
RMSE	0.011	2.138	0.089
MBE	NA	0.3874	0.009
MAE	0.074	1.781	0.17

5. Conclusions and Limitations

In this study, we collected data from three different types of solar panels for the city of Duzce in Turkey and trained an ANN and an LSTM to accurately predict the solar radiation using PV historical data as well as meteorological data. Data were collected for the years between 2014 and 2018 on a daily basis with a 5-min interval. The first model was an ANN model which is frequently used for solar prediction according to the literature. The second model was LSTM which is based on RNNs and is getting more utilization in time series forecasting studies. In the proposed study, we demonstrate the feasibility of accurately predicting solar radiation after 24 h if 15 h of PV historical data along with one previous day of meteorological data are provided to the LSTM. The ability of the LSTM to utilize the historical values of the features allows it to outperform other deep learning models in time series applications. Moreover, we conducted a comparison between our results and similar work in the literature in terms of many error metrics.

Two main limitations of the proposed study would be training the models on data collected solely from the city of Duzce in Turkey. For future work, we plan to collect data from different places in Turkey, or around the globe if possible, to study the generalizability of a trained LSTM model to be used as a prediction tool for solar radiation in different locations. We are aware of the fact that the weather in Duzce is stable most of the time and it perhaps assisted in creating a very accurate model; thus, we are planning to acquire data from places where the weather is more turbulent.

Author Contributions: Conceptualization, T.O. and B.O.A.; methodology, T.O.; software, T.O. and B.O.A.; validation, J.M.Z. and O.T.O.; formal analysis, J.M.Z. and O.T.O.; investigation, T.O.; resources, T.O.; data curation, T.O. and B.O.A.; writing—original draft preparation, T.O.; writing—review and editing, T.O., F.T. and J.M.Z.; visualization, T.O.; supervision, J.M.Z. and O.T.O.; project administration, T.O.; funding acquisition, The Scientific and Technological Research Council of Turkey (TUBITAK). All authors have read and agreed to the published version of the manuscript.

Funding: This research was funded by The Scientific and Technological Research Council of Turkey (TUBITAK), grant number 1059B141800505.

Institutional Review Board Statement: Not applicable.

Informed Consent Statement: Not applicable.

Data Availability Statement: Data utilized in this study were obtained from the Duzce University using the aforementioned described solar panels. Those solar panels were installed in the Duzce University for scientific research in 2013. Data were recorded and saved in the Duzce University database. Moreover, meteorological data were obtained via a protocol between the physics department, Duzce University, and the Ministry of Metrology in Turkey. Data are available upon request.

Acknowledgments: This study was supported by 1059B141800505 from The Scientific and Technological Research Council of Turkey (TUBITAK).

Conflicts of Interest: There is no conflict of interest.

References

1. Husain, A.A.; Hasan, W.Z.W.; Shafie, S.; Hamidon, M.N.; Pandey, S.S. A review of transparent solar photovoltaic technologies. *Renew. Sustain. Energy Rev.* **2018**, *94*, 779–791. [CrossRef]
2. Shahsavari, A.; Akbari, M. Potential of solar energy in developing countries for reducing energy-related emissions. *Renew. Sustain. Energy Rev.* **2018**, *90*, 275–291. [CrossRef]
3. Wang, Z.; Song, H.; Liu, H.; Ye, J. Coupling of solar energy and thermal energy for carbon dioxide reduction: Status and prospects. *Angew. Chem. Int. Ed.* **2020**, *59*, 8016–8035. [CrossRef]
4. Zhang, Y.; Jing, R.; Yanru, P.; Wang, P. Solar energy potential assessment: A framework to integrate geographic, technological, and economic indices for a potential analysis. *Renew. Energy* **2020**, *149*, 577–586. [CrossRef]
5. Rabaia, M.K.H.; Abdelkareem, M.A.; Sayed, E.T.; Elsaid, K.; Chae, K.; Wilberforce, T.; Olabi, A.G. Environmental impacts of solar energy systems: A review. *Sci. Total Environ.* **2021**, *754*, 141989. [CrossRef]
6. Li, J.; Huang, J. The expansion of China's solar energy: Challenges and policy options. *Renew. Sustain. Energy Rev.* **2020**, *132*, 110002. [CrossRef]
7. Grubler, A.; Wilson, C.; Bento, N.; Boza-Kiss, B.; Krey, V.; McCollum, D.L.; Rao, N.D.; Riahi, K.; Rogelj, J.; De Stercke, S.; et al. A low energy demand scenario for meeting the 1.5 C target and sustainable development goals without negative emission technologies. *Nat. Energy* **2018**, *3*, 515–527. [CrossRef]
8. Shamshirband, S.; Rabczuk, T.; Chau, K.W. A survey of deep learning techniques: Application in wind and solar energy resources. *IEEE Access* **2019**, *7*, 164650–164666. [CrossRef]
9. Bildirici, M.E.; Gökmenoğlu, S.M. Environmental pollution, hydropower energy consumption and economic growth: Evidence from G7 countries. *Renew. Sustain. Energy Rev.* **2017**, *75*, 68–85. [CrossRef]
10. Franco, S.; Mandla, V.R.; Rao, K.R.M. Urbanization, energy consumption and emissions in the Indian context A review. *Renew. Sustain. Energy Rev.* **2017**, *71*, 898–907. [CrossRef]
11. Jebli, M.B.; Youssef, S.B. The role of renewable energy and agriculture in reducing CO_2 emissions: Evidence for North Africa countries. *Ecol. Indic.* **2017**, *74*, 295–301. [CrossRef]
12. Nabavi-Pelesaraei, A.; Hosseinzadeh-Bandbafha, H.; Qasemi-Kordkheili, P.; Kouchaki-Penchah, H.; Riahi-Dorcheh, F. Applying optimization techniques to improve of energy efficiency and GHG (greenhouse gas) emissions of wheat production. *Energy* **2016**, *103*, 672–678. [CrossRef]
13. Jebli, I.; Belouadha, F.Z.; Kabbaj, M.I.; Tilioua, A. Prediction of solar energy guided by pearson correlation using machine learning. *Energy* **2021**, *224*, 120109. [CrossRef]
14. Smil, V. *Energy and Civilization: A History*; MIT Press: Cambridge, MA, USA, 2018.
15. Shezan, S.; Julai, S.; Kibria, M.; Ullah, K.; Saidur, R.; Chong, W.T.; Akikur, R. Performance analysis of an off-grid wind-PV (photovoltaic)-diesel-battery hybrid energy system feasible for remote areas. *J. Clean. Prod.* **2016**, *125*, 121–132. [CrossRef]
16. Antonanzas, J.; Osorio, N.; Escobar, R.; Urraca, R.; Martinez-de-Pison, F.J.; Antonanzas-Torres, F. Review of photovoltaic power forecasting. *Sol. Energy* **2016**, *136*, 78–111. [CrossRef]
17. Ahmad, M.J.; Tiwari, G.N. Solar radiation models—A review. *Int. J. Energy Res.* **2011**, *35*, 271–290. [CrossRef]
18. Pandey, A.K.; Tyagi, V.; Selvaraj, J.A.; Rahim, N.; Tyagi, S. Recent advances in solar photovoltaic systems for emerging trends and advanced applications. *Renew. Sustain. Energy Rev.* **2016**, *53*, 859–884. [CrossRef]

19. Wang, F.; Mi, Z.; Su, S.; Zhao, H. Short-Term Solar Irradiance Forecasting Model Based on Artificial Neural Network Using Statistical Feature Parameters. *Energies* **2012**, *5*, 1355–1370. [CrossRef]
20. Su, Y.; Chan, L.-C.; Shu, L.; Tsui, K.-L. Real-time prediction models for output power and efficiency of grid-connected solar photovoltaic systems. *Appl. Energy* **2012**, *93*, 319–326. [CrossRef]
21. Malvoni, M.; Leggieri, A.; Maggiotto, G.; Congedo, P.; de Giorgi, M.G. Long term performance, losses and efficiency analysis of a 960 kW P photovoltaic system in the Mediterranean climate. *Energy Convers. Manag.* **2017**, *145*, 169–181. [CrossRef]
22. Ghazi, S.; Ip, K. The effect of weather conditions on the efficiency of PV panels in the southeast of UK. *Renew. Energy* **2014**, *69*, 50–59. [CrossRef]
23. Salimi, H.; Ashtiani, H.A.D.; Lavasani, A.M.; Fazaeli, R. Experimental analysis and modeling of weather condition effects on photovoltaic systems' performance: Tehran case study. *Energy Sources Part A Recovery Util. Environ. Eff.* **2020**, *7*, 1–13. [CrossRef]
24. Hachicha, A.A.; Al-Sawafta, I.; Said, Z. Impact of dust on the performance of solar photovoltaic (PV) systems under United Arab Emirates weather conditions. *Renew. Energy* **2019**, *141*, 287–297. [CrossRef]
25. Mellit, A.; Pavan, A.M.; Lughi, V. Short-term forecasting of power production in a large-scale photovoltaic plant. *Sol. Energy* **2014**, *105*, 401–413. [CrossRef]
26. Ogliari, E.; Dolara, A.; Manzolini, G.; Leva, S. Physical and hybrid methods comparison for the day ahead PV output power forecast. *Renew. Energy* **2017**, *113*, 11–21. [CrossRef]
27. Benghanem, M.; Mellit, A.; Alamri, S. ANN-based modelling and estimation of daily global solar radiation data: A case study. *Energy Convers. Manag.* **2009**, *50*, 1644–1655. [CrossRef]
28. Mellit, A.; Pavan, A.M. A 24-h forecast of solar irradiance using artificial neural network: Application for performance prediction of a grid-connected PV plant at Trieste, Italy. *Sol. Energy* **2010**, *84*, 807–821. [CrossRef]
29. Voyant, C.; Muselli, M.; Paoli, C.; Nivet, M.-L. Numerical weather prediction (NWP) and hybrid ARMA/ANN model to predict global radiation. *Energy* **2012**, *39*, 341–355. [CrossRef]
30. Sözen, A.; Arcaklioğlu, E.; Özalp, M. Estimation of solar potential in Turkey by artificial neural networks using meteorological and geographical data. *Energy Convers. Manag.* **2004**, *45*, 3033–3052. [CrossRef]
31. Mellit, A.; Shaari, S. Recurrent neural network-based forecasting of the daily electricity generation of a Photovoltaic power system. *Ecol. Veh. Renew. Energy (EVER)* **2009**, 26–29. Available online: http://citeseerx.ist.psu.edu/viewdoc/download?doi=10.1.1.533.9274&rep=rep1&type=pdf (accessed on 1 September 2019).
32. de Araujo, J.M.S. Performance comparison of solar radiation forecasting between WRF and LSTM in Gifu, Japan. *Environ. Res. Commun.* **2020**, *2*, 045002. [CrossRef]
33. Alzahrani, A.; Shamsi, P.; Dagli, C.; Ferdowsi, M. Solar Irradiance Forecasting Using Deep Neural Networks. *Procedia Comput. Sci.* **2017**, *114*, 304–313. [CrossRef]
34. Rai, A.; Shrivastava, A.; Jana, K.C. A CNN-BiLSTM based deep learning model for mid-term solar radiation prediction. *Int. Trans. Electr. Energy Syst.* **2020**, *31*, e12664. [CrossRef]
35. Yousif, J.H.; Kazem, H.A.; Alattar, N.N.; Elhassan, I.I. A comparison study based on artificial neural network for assessing PV/T solar energy production. *Case Stud. Therm. Eng.* **2019**, *13*, 100407. [CrossRef]
36. Jung, Y.; Jung, J.; Kim, B.; Han, S.U. Long short-term memory recurrent neural network for model in temporal patterns in long-term power forecasting for solar PV facilities: Case study of South Korea. *J. Clean. Prod.* **2020**, *250*, 119476. [CrossRef]
37. Mishra, M.; Dash, P.B.; Nayak, J.; Naik, B.; Swain, S.K. Deep learning and wavelet transform integrated approach for short-term solar PV power prediction. *Measurement* **2020**, *166*, 108250. [CrossRef]
38. Ghimire, S.; Deo, R.C.; Raj, N.; Mi, J. Deep solar radiation forecasting with convolutional neural network and long short-term memory network algorithms. *Appl. Energy* **2019**, *253*, 113541. [CrossRef]
39. Lee, D.; Kim, K. Recurrent Neural Network-Based Hourly Prediction of Photovoltaic Power Output Using Meteorological Information. *Energies* **2019**, *12*, 215. [CrossRef]
40. Pang, Z.; Niu, F.; O'Neill, Z. Solar radiation prediction using recurrent neural network and artificial neural network: A case study with comparisons. *Renew. Energy* **2020**, *156*, 279–289. [CrossRef]
41. Gensler, A.; Henze, J.; Sick, B.; Raabe, N. Deep Learning for solar power forecasting—An approach using AutoEncoder and LSTM Neural Networks. In Proceedings of the 2016 IEEE International Conference on Systems, Man, and Cybernetics (SMC), Budapest, Hungary, 9–12 October 2016; pp. 002858–002865.
42. Bakirci, K. Models of solar radiation with hours of bright sunshine: A review. *Renew. Sustain. Energy Rev.* **2009**, *13*, 2580–2588. [CrossRef]
43. Chen, Y.; Lin, M.; Yu, R.; Wang, T. Research on Simulation and State Prediction of Nuclear Power System Based on LSTM Neural Network. *Sci. Technol. Nucl. Install.* **2021**, *2021*, 8839867. [CrossRef]
44. Zhou, N.; Ren, N.; Zhou, J.; Huang, C. Prediction of remaining mileage of hydrogen energy vehicles based on LSTM. In Proceedings of the 2021 4th International Conference on Advanced Electronic Materials, Computers and Software Engineering (AEMCSE), Changsha, China, 26–28 March 2021; pp. 749–753.
45. Turkish State Meteorological Service Official Web Sites. Available online: https://mgm.gov.tr/eng/forecast-cities.aspx (accessed on 1 September 2019).
46. Rosenblatt, F. *The Perceptron: A Perceiving and Recognizing Automaton (Project PARA)*; Report No. 85-460-1; Cornell Aeronautical Laboratory: New York, NY, USA, 1957.

47. Chung, J.; Gulcehre, C.; Cho, K.; Bengio, Y. Empirical Evaluation of Gated Recurrent Neural Networks on Sequence Modeling. In Proceedings of the NIPS 2014 Workshop on Deep Learning, Cornell University, New York, NY, USA, 10 December 2014.
48. Lipton, Z.C.; Berkowitz, J.; Elkan, C. A Critical Review of Recurrent Neural Networks for Sequence Learning. *arXiv* **2015**, arXiv:1506.00019.
49. Goodfellow, I.; Bengio, Y.; Courville, A. *Deep Learning*; MIT Press: Cambridge, MA, USA, 2016.
50. Ghaderi, A.; Sanandaji, B.M.; Ghaderi, F. Deep Forecast: Deep Learning-based Spatio-Temporal Forecasting. *arXiv* **2017**, arXiv:1707.08110.
51. Hochreiter, S.; Schmidhuber, J. Long Short-Term Memory. *Neural Comput.* **1997**, *9*, 1735–1780. [CrossRef]
52. Lee, H.-Y. Deep Learning Neural Network with Memory (1)—PPT Video Online Download. Available online: https://slideplayer.com/slide/7478657/ (accessed on 2 September 2019).
53. Ramachandran, P.; Zoph, B.; Le, Q.V. Searching for Activation Functions. *arXiv* **2017**, arXiv:1710.05941.
54. Nwankpa, C.; Ijomah, W.; Gachagan, A.; Marshall, S. Activation functions: Comparison of trends in practice and research for deep learning. *arXiv* **2018**, arXiv:1811.03378.
55. Sibi, P.; Jones, S.A.; Siddarth, P. Analysis of different activation functions using back propagation neural networks. *J. Theor. Appl. Inf. Technol.* **2013**, *47*, 5.
56. Sharma, S. Activation functions in neural networks. *Towards Data Sci.* **2017**, *6*, 310–316. [CrossRef]
57. Karlik, B.; Olgac, A.V. Performance analysis of various activation functions in generalized MLP architectures of neural networks. *Int. J. Artif. Intell. Expert Syst.* **2011**, *1*, 111–122.
58. Cheng, J.; Dong, L.; Lapata, M. Long Short-Term Memory-Networks for Machine Reading. *arXiv* **2016**, arXiv:1601.06733.
59. Zurada, J.M. *Introduction to Artificial Neural Systems*; West: Eagan, MN, USA, 1992.
60. Ağbulut, U.; Gürel, A.E.; Biçen, Y. Prediction of daily global solar radiation using different machine learning algorithms: Evaluation and comparison. *Renew. Sustain. Energy Rev.* **2021**, *135*, 110114. [CrossRef]